Anal. Bioanal. Electrochem., Vol. 15, No. 1, 2023, 17-35
https://www.doi.org/ 10.22034/abec.2023.701392

Analytical & Bioanalytical Electrochemistry

Full Paper

The Inhibiting Effect of Aqueous Extracts of Artemisia Absinthium L. (Wormwood) on the Corrosion of Mild Steel in HCl 1 M

A. Hbika,[1] A. Bouyanzer,[1] M. Jalal,[1] N. Setti,[2] E. Loukili,[1] A. Aouniti,[1] Y. Kerroum,[3] I. Warad,[4] B. Hammouti,[1] and A. Zarrouk[3,*]

[1]*Laboratory of Applied and Environmental Chemistry (LCAE), Team Applied Analytical Chemistry of Materials and Environment, Mohammed First University, Faculty of Science, Department of Chemistry, 60000 Oujda, Morocco*
[2]*Laboratory of Applied and Environmental Chemistry (LCAE), Electrochemical team, Mohammed First University, Faculty of Science, Department of Chemistry, 60000 Oujda, Morocco*
[3]*Laboratory of Materials, Nanotechnology and Environment, Faculty of Sciences, Mohammed V University in Rabat, Av. Ibn Battouta, P.O. Box 1014 Agdal-Rabat, Morocco*
[4]*Department of Chemistry, AN-Najah National University, P.O. Box 7, Nablus, Palestine*

*Corresponding Author, Tel.: +212665201397
E-Mail: azarrouk@gmail.com

Received: 20 December 2022 / Accepted with minor revision: 23 January 2023 / Published online: 31 January 2023

Abstract- Using the decoction extraction method, we obtained twice crude aqueous extracts of Artemisia absinthium or (wormwood) that was made to start a comparative study, between the first extract which corresponds to the leaves of our plant (AQL) and the second which belongs to the stems (AQS). The inhibitory activity of the twice extracts of Artemisia absinthium was studied by weight loss, potentiodynamic polarization and electrochemistry impedance spectroscopy. The morphology of the mild steel surface was examined by SEM. The inhibitory efficiency increased with the increase of the concentration, we reach an efficiency of 85% for AQL and 82% for AQS at 308 K for a concentration of 0.2 g/L. Two Artemisia absinthium extracts used to prevent corrosion in mild steel adhere to the Langmuir adsorption isotherm during adsorption. The majority compound is 3,4-dihydroxybenzoic acid in the case of extracts with percentages of 42.4% for AQL and 42.2% for AQS. The DFT results of the majority of compounds allowed us to have an idea on the power of adsorption of these last ones on the surface of the metal, indeed there can be a combined effect of the various molecules constituting the extracts on the corrosion inhibition.

Keywords- Artemisia absinthium; Aqueous extracts; Mild steel; Corrosion inhibition; DFT

1. INTRODUCTION

Corrosion is a natural and spontaneous process like the fall of anything from top to bottom due to gravity or like the further increase of entropy in the universe, if we speak at the level of the energy, the presence of oxygen and water in all kinds of environment causes iron to combine with atoms of oxygen and hydrogen to form iron oxide to return to their states of lowest energy [1]. If you type the word corrosion on the internet or look for it in books, you will find many definitions, some short ones do not fully explain this phenomenon, others specifically explain the different cases of corrosion by explaining the forms of degradation material like galvanic corrosion, uniform corrosion, pitting corrosion, intergranular corrosion and crevice corrosion. For this, corrosion as a natural phenomenon can be defined as an irreversible process between a substance and the surrounding environment that controls the types of decomposition of the material [2,3].

Corrosion of materials remains a problem that preoccupies researchers and encourages them to launch initiatives to remedy the destructive effects of this phenomenon which affects the desired function of our material, especially in industries where acid enters the cleaning of machines process [4-6], it is therefore necessary to use inhibitors to minimize the degradation of the metal and increase its lifespan, despite the fact that there are many inhibitors, but finding an inhibitor that does not have adverse effects on our environment is the most important. Most synthetic compounds have good anti-corrosive properties but are highly toxic which can damage organic systems by disrupting biochemical processes and the body's enzyme system [7].

For this reason, we attempted to use the Artemisia absinthium plant's crude aqueous extracts (CAE) as an environmentally friendly inhibitor in the current work. Artemisia absinthium L. is a member of the tribe Anthemideae of the Asteraceae family. It goes by the popular names absinthe in France, wormwood in the United Kingdom, afsantine in Iran, and wennut in Germany [8,9]. In Europe, North Africa, the Middle East, and Asia, it has been utilized in phytotherapy [10]. is a bitter, aromatic herb that has been used for centuries as a multipurpose medicinal. It was a well-liked plant in the Middle Ages, and most herbariums and medical texts mention it. The medication was prescribed as a powder infusion. Antitrypanosomal [11], antibacterial [12], antiplasmodial [13], antipyretic [14], anti-inflammatory and analgesic [15], antidepressant and antifungal [16], and antioxidant impact [17] are just a few of the biological activities that have been assessed .

Under the control of electrochemical and weight loss procedures, this investigation was organized to estimate the inhibitory activity of aqueous crude Artemisia extracts on the corrosion process of mild steel in a cleaning concentration of 1 M hydrochloric acid. The chemical composition of the extracts was identified by high performance liquid chromatography HPLC. To study the form of corrosion and surface morphology, the samples

were inspected by SEM. The majority of compounds of Artemisia absinthium extracts are optimized using density functional theory (DFT).

2. EXPERIMENTAL METHODS

2.1. Inhibitor Extraction

We chose the region of Mestferki which is located almost 25 km from Oujda city (Morocco) to collect a sample of the plant Artemisia absinthium, this harvest was carried out on 13th December 2018. Leaves and stems of *Artemisia absinthium* were freshly collected and dried separately in a dry and ventilated place, protected from light. The dried plant material was ground. The extraction of the leaf and stem powder (100 g) was done separately by decoction with distilled water for 2 hours after the removal of the essential oil.

2.2. High performance liquid chromatography (HPLC)

A liquid chromatography separation module (Waters e2695) connected to a diode array detector (Waters 2998 PDA) and data processing software called Empower was used to perform the HPLC/DAD analysis. Chromatograms between 254 and 300 nm were captured. a C18 column (4.6 mm by 250 mm by 5 μm). The mobile phase was performed in gradient mode using ultrapure water/acetic acid (0.5%) (solvent A) and methanol (solvent B) at flow rates of 1 mL/min and 20 μL for injection volumes, respectively (0 min, 80% A, 20% B; 20 min, 0% A, 100% B; and 25 min, 0% A, 100% B). Retention times and UV spectra were compared to standards, and the results were used to identify the peaks. Gallic acid, vanillic acid, catechin, caffeic acid, rosmarinic acid, p-hydroxy benzoic acid, rutin, quercetin, syringic acid, vanniline, naringenin, P-coumaric acid, Artemetin, Ascorbic acid, ferulic acid, malic acid, and kaempferol were the standard polyphenolic substances employed. These substances had previously been discovered in *Artemisia absinthium.*

2.3. Materials used for corrosion assessment

Basic chemical composition of samples by weight is presented in Table 1, before starting each procedure, the material already described above is polished using a series of emery paper sheets number 180–1200.Then, all the samples used are washed and degreased with distilled water and acetone, respectively, and finally dried.

The 37 percent analytical grade concentrated HCl was mixed with distilled water to obtain the 1 M HCl cleaning solution.The required inhibitor concentrations (in g/L) were dissolved in acid solution, and the inhibitor-free solution served as a baseline for comparison. Before each experiment, the test solutions were freshly made by mixing *Artemisia absinthium* extracts right into the corrosive solution. The extracts used have concentrations of 0.025, 0.05, 0.1, and 0.2 g/L.

Table 1. Basic chemical composition of samples

Elements	Fe	Si	C	Cu	P	S	Al
Percentage	99.12	0.38	0.21	0.14	0.09	0.05	0.01

2.4. Weight loss studies

The metallic iron sample sheets, which measure 1×1×0.2 cm, were scraped before being submerged in 100 mL of acid (1 M HCl) with a range of inhibitor amounts for varying durations. After being removed, they are submerged in an acetone solution to remove any residue. They are then completely washed with tap water, rinsing them with distilled water, and drying them. All measurements were made a few times, and average values were published, in order to achieve good repeatability.

The corrosion rate (C_R), the inhibition efficiency (η_G (%)) and the degree of surface coverage (θ) were calculated as follows [18]:

$$C_R = \frac{(W_b - W_a)}{A \times t} \quad (1)$$

$$\eta_G(\%) = \left(\frac{C_R^O - C_R}{C_R^O} \right) \times 100 \quad (2)$$

$$\theta = \left(\frac{C_R^O - C_R}{C_R^O} \right) \quad (3)$$

where A is the surface area (cm^2), t represents the duration of time it takes to submerge the metal, and W_a and W_b are the sample weights (mg) after the experiment and before it in solutions of hydrochloric acid, respectively. C_R describes the effect of the amount of inhibitor on the corrosion rate of the samples, and C_R^O describes the effect of the blank solution.

2.5. Electrochemical studies

Tacussel corrosion analysis software model (Voltamaster 4) was used to control the Volta lab (Tacussel- Radiometer PGZ 100) potentiostate for the electrochemical measurement studies, which were conducted in a static environment. In a double-walled electrochemical cell with a thermometer, 100 mL of 1 M HCl was added, both without and with various doses of the inhibitor. The electrolyte is maintained at the proper temperature by a thermostat that circulates water. Three electrodes are present in the corrosion cell. a working electrode constructed of mild steel with a surface area of 1 cm^2, a platinum electrode with a surface area of 1 cm^2, and a saturated calomel electrode (SCE), which serves as a reference electrode. The working electrode was submerged in the test solution for 30 minutes to create a steady state open circuit potential. The potentials are relative to the reference electrode (E_{ocp}). The

electrochemical experiments and testing were carried out in aerated solutions at a temperature of 308 K after measuring this potential.

The AC sine wave amplitude used in the EIS studies was 10 mV peak-to-peak at open circuit potential, and the frequency range used was 100 kHz–10 mHz [19,20]. These tests produced nyquist plots, which were then used to evaluate and extract impedance data. The following equation determines the proportion of inhibitory effectiveness from the impedance diagrams [21,22]:

$$\eta_{EIS}\left(\%\right)=\left(\frac{R_p-R_p^O}{R_p}\right)\times 100 \tag{4}$$

where R_p and R_p^O are the polarization resistances in the presence and absence of inhibitor in the corrosive solution. Potentiodynamic polarization measurements were recorded from both cathodic and anodic directions with a scan rate of 0.5 mVs^{-1} by changing the electrode potential automatically from -800 to -200 [23,24]. The cathodic and anodic linear segments of the Tafel curves were extrapolated to the corrosion potential to obtain the corrosion current densities (i_{corr}). The percent inhibitory efficiency from the polarization curves η_{pc} (%) is determined as follows [25,26]:

$$\eta_{PC}\left(\%\right)=\left(\frac{i_{corr}^O-i_{corr}}{i_{corr}^O}\right)\times 100 \tag{5}$$

where i_{corr} and i_{corr}^O are the current densities in the presence and absence of inhibitor in the corrosive solution.

2.6. Surface examination study

The morphology composition of mild steel in 1M HCl solution in the presence and absence of aqueous extracts of *Artemisia absinthium* for an optimal concentration (0.2g/L) were analyzed after 24 hours of immersion by scanning electron microscopy (SEM) using a JEOL JSM-IT500HR apparatus. The aluminum sample holder held the mild steel samples while they were being inspected at an 8 kV accelerating voltage.

2.7. Computational studies

Density function theory (DFT) was used to completely optimize the geometries of the majority of the compounds in the aqueous extracts of Artemisia absinthium. The hybrid function B3LYP was employed, and the theoretical calculations at this level of DFT/B3LYP theory were carried out using the 6-31G (d,p) [27] basis implemented in the Gaussian 09W software suite, which supports electronic structure modeling. These calculations have shown to be an effective technique to understand how corrosion inhibition works. Total energy (ET), lowest unoccupied molecular orbital energy (E_{LUMO}), highest molecular orbital energy

(E_{HOMO}), and other characteristics can be estimated using the formulae shown in Table 2 to describe the global reactivity of the principal components in *Artemisia absinthium* extracts.

Table 2. Equations of quantum parameters descriptors of global reactivity

Global reactivity descriptors	Equation
Energy gap	$\Delta E_{gap} = E_{LUMO} - E_{HOMO}$
Absolute electronegativity	$\chi = (I+A)/2$
Global hardness	$\eta = (I - A)/2$
Fraction of emitted electrons	$\Delta N = (\varphi_{metal} - \chi)/\eta$

I: Ionization potential ($I = -E_{HOMO}$), A: Electron affinity ($A = -E_{LUMO}$), φ_{metal}: work function of metal (φ_{metal} = 4.81 eV**)**

3. RESULTS AND DISCUSSION

3.1. HPLC analysis of the extracts

By contrasting their retention times and UV spectra, high performance liquid chromatography linked to a diode array detector (HPLC-DAD) was used to determine the chemical composition of *Artemisia absinthium* aqueous extracts. The chromatograms of aqueous leaf extract (AQL) and aqueous stem extract (AQS) are shown in Figure. 1 and 2 respectively. Figure.3 shows the chemical structures of the compounds identified in these two extracts.

The most abundant compound was 3,4-Dihydroxybenzoic acid with almost identical percentages of 42.4% and 42.2% for AQL and AQS respectively. AQL contains also Gallic acid (14.40%), Vanillin (13.73%), Catechin hydrate (10.31%), Naringenin (8.96%), Malic acid (4.30%) and Ascorbic acid (1.30%). Also the presence of Vanillin (15.91%), Naringenin (11.83%), Gallic acid (7.60%), 4-Hydroxybenzoic acid (3.44%), Vanillic acid (3.16%), Caffeic acid (3.05%) and Ascorbic acid (1.55%) in AQS.

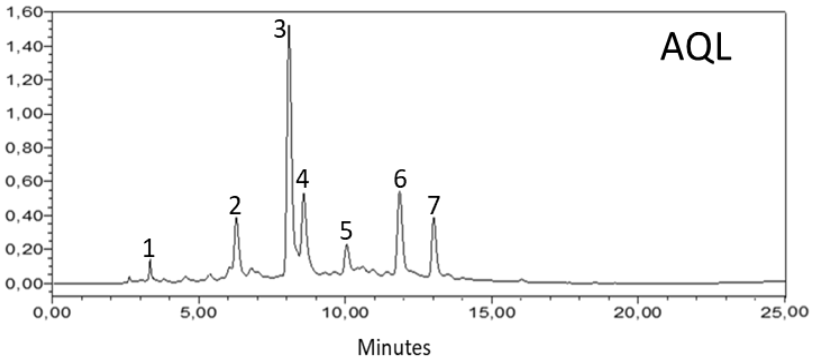

Figure 1. HPLC chromatograms patterns of AQL: ((1) Ascorbic acid (1.30 %), (2) Catechin Hydrate (10.31%), (3) 3,4-Dihydroxybenzoic acid (42.4 %), (4) Gallic acid (14.40 %), (5) Malic acid (4.30 %), (6) Vanillin (13.73%) and (7) Naringenin (8.96 %))

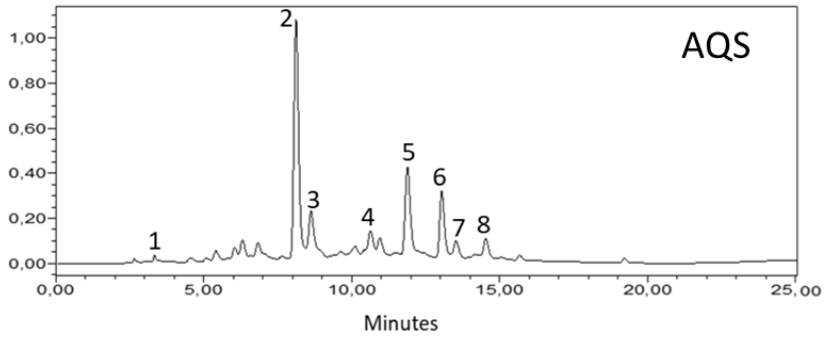

Figure 2. HPLC chromatograms patterns of AQS: ((1) Ascorbic acid (1.55 %), (2) 3,4-Dihydroxybenzoic acid (42.2%), (3) Gallic acid (7.60 %), (4) 4-Hydroxybenzoic acid (3.44 %), (5) Vanillin (15.91%), (6) Naringenin (11.83 %), (7) Vanillic acid (3.16%) and (8) Caffeic acid (3.05%))

Works have reported the presence of these molecules in the extracts of Artemisia absinthium, it has been confirmed the presence of Gallic acid, Caffeic acid [28], vanillic acid [29], Vanillin, Naringenin [30], Malic acid [31], Ascorbic acid [32], Catechin [33], 4-hydroxybenzoic acid [34] and Protocatechuic acid or 3,4-Dihydroxybenzoic acid [35]. This plant was established for production of commercially important secondary metabolites [36].

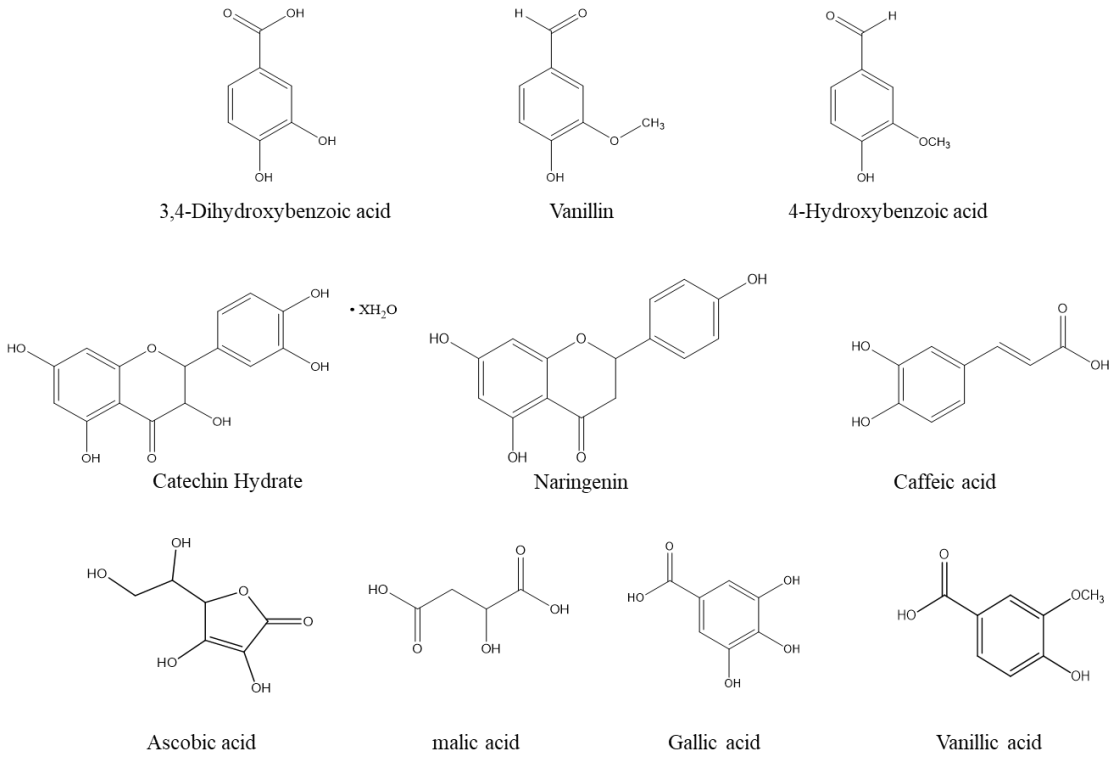

Figure 3. Compounds found in aqueous extracts of artemisia absinthium

3.2. Weight loss method

Different amounts of AQL and AQS were tested to establish the degree of corrosion of the samples at different concentrations during 6 hours of immersion at a temperature of 308K. Table 3 shows the values of corrosion rates, inhibitory efficiencies and metal surface coverage rates achieved by the gravimetric method. The addition of the extracts remarkably decreased the corrosion rate, as well as a clear dependence between this rate and the concentration of the *Artemisia absinthium* extracts. AQL and AQS show corrosion inhibition efficiencies of 88.8% and 88.2% respectively for a maximum concentration of 0.2 g/L.

It is observed that the inhibition effect is improved with the increment of the concentration, this translates into a reduction of the chemical attacks coming from the HCl medium,which is probably caused by the formation of a film of the extract molecules on the mild steel surface when the extract concentration is increased. A better inhibition efficiency was noticed for AQL, this effect can be a sign of effective coverageof the metal by the molecules from this extract.

In general, the active sites of the extraction molecules can occupy an essential role in the process of adsorption of these molecules on the metal surface, indeed the presence of hydroxyl groups in 3,4-hydroxybenzoic acid Vanillin, naringenin and gallic acid in Artemisia absinthium extracts contributes effectively to the adsorption of the inhibitor and thus to the corrosion inhibition of mild steel. They may contribute to the adsorption of the inhibitor and thus to the inhibition of corrosion of mild steel.

So these molecules have the ability to donate electrons activating electron pairs on the oxygen atoms which increases electron density on the benzene ring.in fact It has been reported that plant extracts with heterocycle compounds can be used as corrosion inhibitors, as they can easily adsorb onto the metal surface because of their aromatic rings, free electrons, pi bonds (π bonds) as well as polar functional groups that serve as adsorption centres [37].

Table 3. Inhibition effect with increasing AQL and AQS concentrations after 6 hours of immersion in HCl

	Concentration (g/L)	Corrosion rate CR (mg $cm^{-2}h^{-1}$)	Inhibition efficiency η_G (%)	Surface coverage θ
Blank	0	0.750	-----	-----
AQL	0.2	0.084	88.8	0.888
	0.1	0.104	86.1	0.861
	0.05	0.213	71.6	0.716
	0.025	0.290	61.3	0.613
AQS	0.2	0.088	88.3	0.883
	0.1	0.201	73.2	0.732
	0.05	0.367	51.1	0.511
	0.025	0.436	41.9	0.419

3.3. Langmuir adsorption isotherm

The basic information about the interaction between the extract molecules and and the mild steel surface can be explicated by an adsorption isotherm. The inhibitory effectiveness and interaction of the molecules on the mild steel surface depends principally on the adsorption of the inhibitor molecules on the electrode surface [38].

The surface coverage values (θ) calculated from the weight loss method as a function of inhibitor concentration were traced by fitting to the Langmuir isotherm, the equation that plots the Langmuir isotherm is as follows[39,40]:

$$\frac{\theta}{1-\theta} = K_{ads}\, C \qquad (6)$$

where C is the concentration of the inhibitor in the solution and K_{ads} is the adsorption-desorption equilibrium constant.

The curves obtained from the Langmuir isotherm equation at different temperatures for AQL and AQS are linear with correlation coefficients of 0.9995 and 0.96 respectively (Figure 4), this shows that the adsorption of Artemisia absinthium extracts on the surface of mild steel in 1 M HCl medium obeys the Langmuir adsorption isotherm.

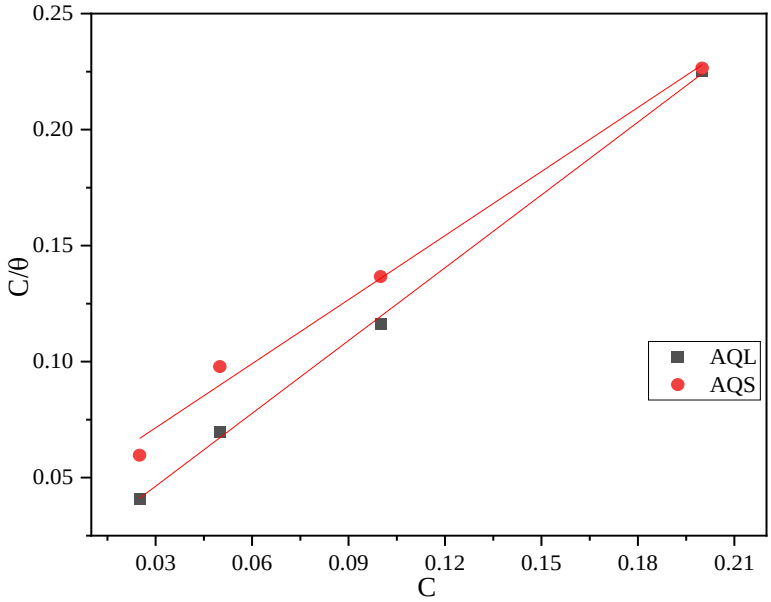

Figure 4. Effect of AQL and AQS concentrations on the Langmuir's adsorption isotherm at 303 K

3.4. Electrochemical impedance spectroscopy studies

The impedance diagrams were plotted in order to search the trend of parameters for the electrochemical resistance of the substrate system and 1 M HCl at various concentrations of AQL and AQS extracts, the measurements were produced and presented in Figure 5 and Figure

6. Then, the impedance properties of the system are represented as the polarization resistance (R_p), the double-layer capacitance (C_{dl}), and the efficiency inhibitor in Table 4.

Furthermore, the AQL and AQS extracts enhance the diameters of the capacitive loops to more elevated values than that of the blank solution, remarkably this increase becomes more marked when the concentration of these extracts increases. The Nyquist plots include animperfect capacitive loop for each solution, which justifies that the corrosion process was principally controlled by charge transfer. Moreover, these imperfect semicirclesmay be a result of the difference in frequency dispersion [41], or the heterogeneity of the electrochemical system resulting from impurities, surface roughness and the formation of porous inhibitor layers [42,43].

Besides, the decline of C_{dl} value when adding AQL and AQS may explain that the adsorption of these extracts occurs at the active sites of the samples [44], The addition of AQL and AQS to the system decreases considerably the values of the capacity of the double layer in fact it passes from 167.5 μFcm^{-2} to 78.70 and 89.77 μFcm^{-2} for AQL and AQS respectively for a concentration of 0.2g/L, this transition can be described as the adsorption of the active organic molecules of the extracts on the active sites of the samples, according to the Helmholtz model, the greater the adsorption of the inhibitor on the metal surface, the thicker the organic matter deposited (e) and the more the capacity of the double layer (C_{dl}) decreases. The increase in polarization resistance (R_p) leads to the increase in inhibitory efficiency. An efficiency of 85.1% is obtained in the case of mild steel inhibition by AQL and 81.9% at concentration of 0.2 g/L.

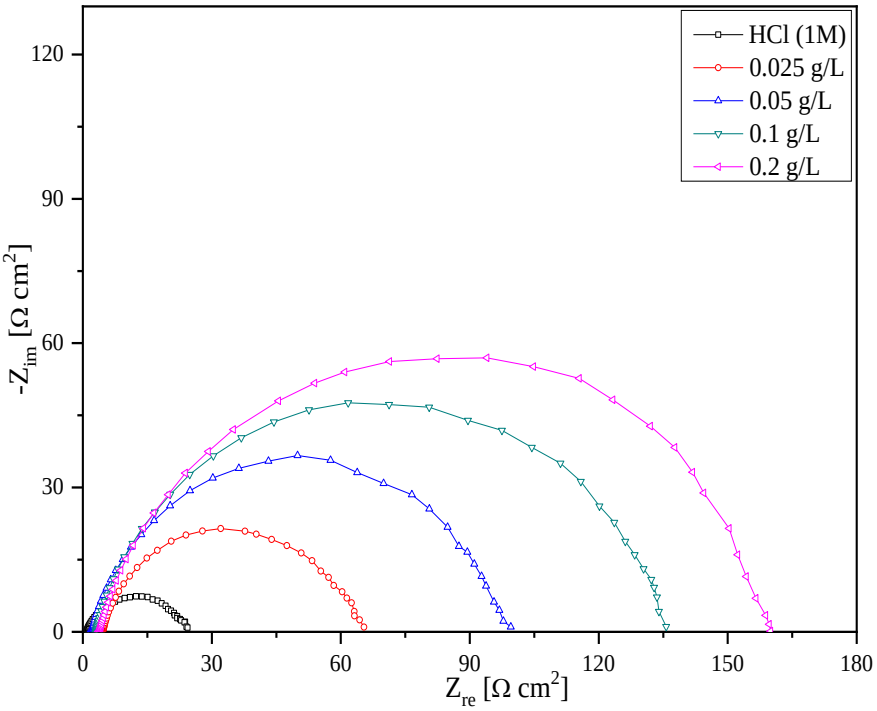

Figure 5. Effect of AQL concentrations on the Nyquist plots at 308 K

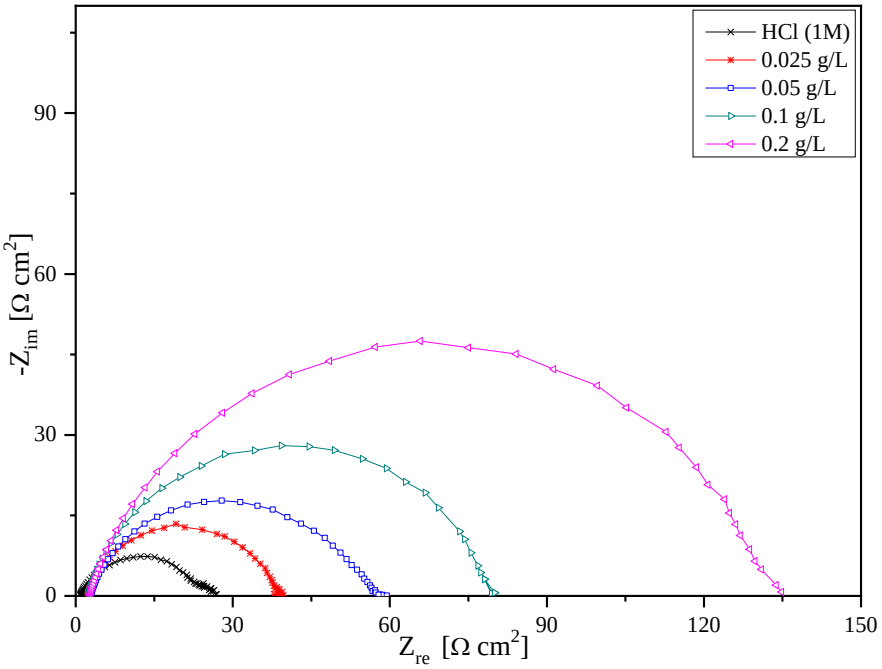

Figure 6. Effect of AQS concentrations on the Nyquist plots at 308 K

Table 4. Effect of AQL and AQS concentrations on the impedance parameters at 303 K

	Concentration (g/L)	R_p	C_{dl} (μFcm^{-2})	η_{EIS} (%)
Blank	-	24.5	167.5	-
AQL	0.2	164.3	78.7	85.1
	0.1	136.4	83.5	82.0
	0.05	96.8	95.2	74.7
	0.025	63.5	101.4	61.4
AQS	0.2	135.3	89.8	81.9
	0.1	80.8	98.9	69.7
	0.05	54.6	108.0	55.0
	0.025	39.4	113.7	37.7

3.5. Potentiodynamic polarization studies

Figure 7 and Figure 8 display the effect of AQL and AQS on the polarization curves of samples in HCl solution, respectively at 303 K, and Table 5 presents the parameters describing the interpretation of the corrosion mechanism such as the potential (E_{corr}), and the current density (i_{corr}), in the same direction, anodic and cathodic Tafel slope (β_a) and (β_c) were extracted from Tafel polarization diagrams.

The addition of AQL and AQS extracts in HCl solutions reduces the cathodic and anodic current density of the substrates, and this decline correlated with the concentrations, indicating that the Artemisia Absinthium extracts were effectively adsorbed at the active sites of the samples.

Moreover, the anodic and cathodic portions of the curves, shift towards lower current densities when adding and increasing the concentration of the extracts, in another way, the addition of these extracts obviously affects the cathodic and anodic curves. These results confirm the dual action of AQL and AQS inhibitors, which can be classified as a mixed type with a cathodic orientation. Besides, lower in the corrosion current density leads to higher inhibition efficiency.A maximum inhibition of 90.5 % is reached for AQL and 85.3% for AQS at 0.2 g/L. On the other hand, reaches an efficiency of 66.9 % in the presence of AQL and 37.8 % in the presence of AQS for a low concentration (0.025 g/L). The cathodic and anodic Tafel slopes changed, which implies that the cathodic hydrogen evolution and the anodic metal dissolution reaction took place.

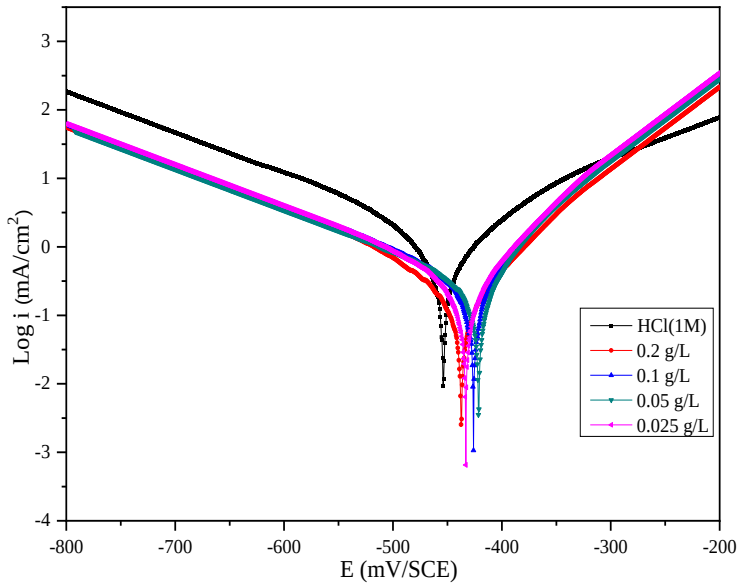

Figure 7. Effect of AQL concentrations on the polarization curves at 303K

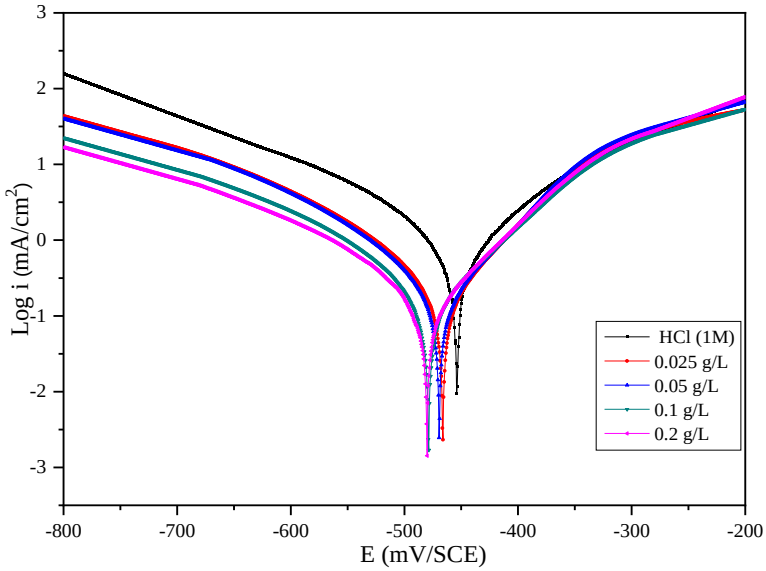

Figure 8. Effect of AQS concentrations on the polarization curves at 303K

Table 5. Effect of AQL and AQS concentrations on the corrosion parameters at 303 K.

	Concentration (g/L)	E_{corr} (mV/SCE)	$-\beta_c$ (mV/dec)	β_a (mV/dec)	i_{corr} (mA/cm²)	η_{PC} (%)
Blank	-	-453.5	179.9	149.1	1.882	-
AQL	0.2	-437.3	107.0	70.7	0.178	90.5
	0.1	-425.6	157.2	68.0	0.316	83.2
	0.05	-421.8	193.3	70.0	0.373	80.1
	0.025	-433.4	211.4	86.4	0.622	66.9
AQS	0.2	-479.6	146.3	89.5	0.275	85.4
	0.1	-478.7	187.4	117.0	0.595	68.4
	0.05	-469.4	176.7	1112	0.839	55.4
	0.025	-466.2	222.0	130.7	1.170	37.8

3.6. Surface studies

The analysis of the mild steel surface by scanning electron microscope was performed in order to have some idea on the morphology of the mild steel surface. Figure 9 shows the Meb images obtained before immersion and after 24 h of immersion in 1M HCl solutions in the absence and presence of 0.2 g/L and AQL and AQS extract.

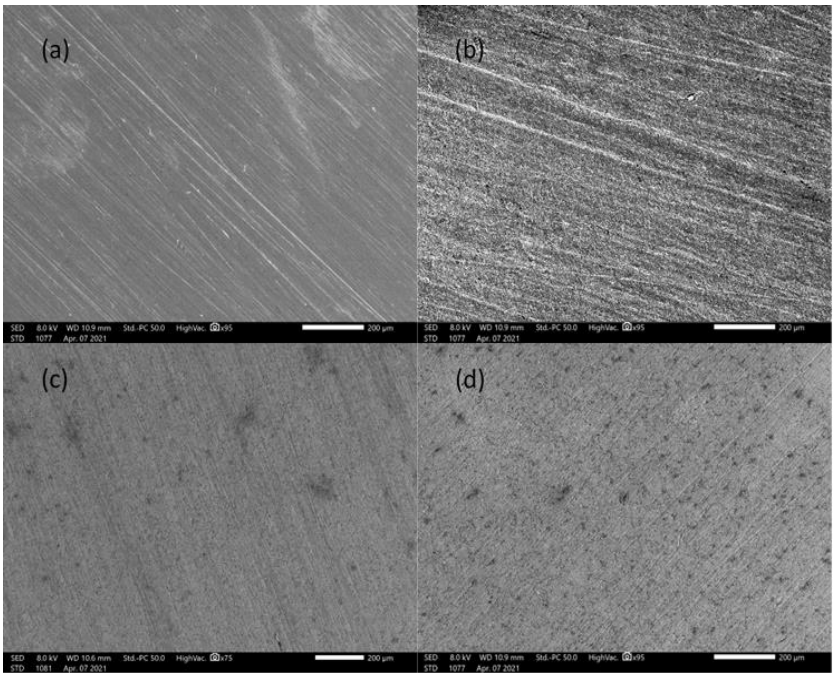

Figure 9. Effect of AQL and AQS on the SEM micrographs of the sample surface **a**) polished surface **b**) 1M HCl and **c**) 1M HCl + aqueous leaf extract and **d**) 1M HCl + aqueous stem extract

It can be clearly seen that the surface of mild steel before immersion in HCl solution (Figure 9-a) is obviously different from that in the absence or presence of Artemisia absinthium extracts

which is remarkably corroded. Figure 9-b shows that the surface of mild steel immersed in HCl in the absence of extracts was strongly damaged which can be justified by the presence of H^+ and Cl^- ions, coming from excessive dissolution of mild steel in HCl medium. The addition of AQL (Figure 9-c) and AQS (Figure 9-d) to the corrosive solution allowed to obtain smoother mild steel surfaces and to minimize and reduce the damage caused by corrosion on its surface, in fact the latter is remarkably less damaged, this result can be attributed to the formation of an inhibitor film that reduces the dissolution of the metal in the presence of HCl ref. From these images it is clear that AQL provides better corrosion protection than AQS, as confirmed by the previous methods.

3.7. Quantum chemical studies

In order to have an idea on the molecules which contributed to the corrosion inhibition, a theoretical study by the density function theory (DFT) was carried out by the B3LYP method using the 6-311G (d, p) base. This study was carried out to determine the molecules responsible for the difference in inhibitory efficiency found between AQL and AQS, knowing that the majority compound was the same in the case of these two extracts with almost equal percentages, also to describe the interaction between the inhibitor molecules and the metal surface, although the properties of the activity of these molecules, in addition it allows to give an idea of the molecules responsible for the inhibitory effect in the case of plant extracts.

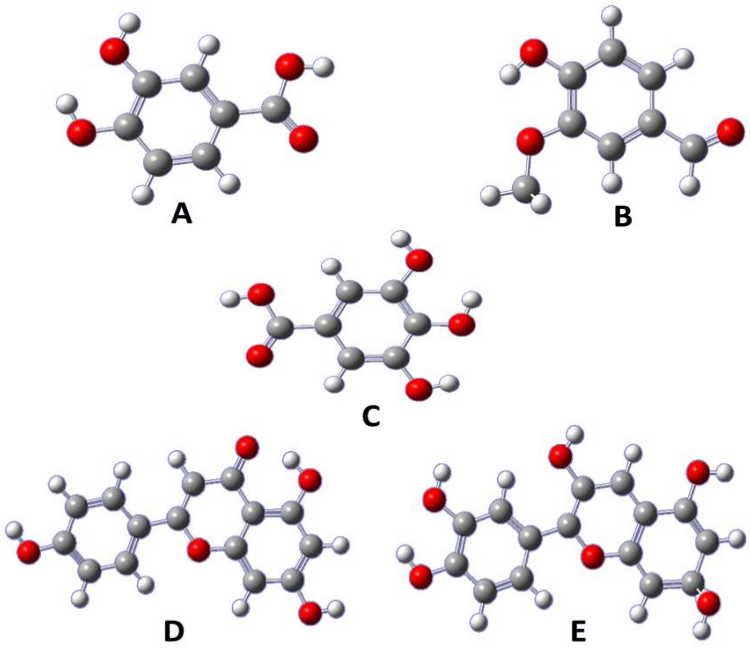

Figure 10. Optimization geometryof 3,4-dihydroxybenzoic acid (A), vanillin (B), gallic acid (C), naringenin (D) and catechine (E) obtained with the DFT at B3LYP/6-31G (d,p) level

Figure 10 shows the optimized geometries of 3,4-dihydroxybenzoic acid (A), Vanillin (B), Gallic acid (C), Naringenin (D) and Catechin (E), and the 3D plots of the ground state boundary orbitals of the HOMO and LUMO energies of these molecules are presented in Figure 11. The quantum descriptors of the molecules were calculated by DFT at B3LYB/6-31G (d, p) and are presented in Table 6. From Figure 11 we can see that the electron densities were distributed on the surface of the whole molecules, and that the higher electron density on HOMO and LUMO suggests that these are the donor and acceptor sites of the inhibitors. These densities are localized on the aromatic rings which are responsible for the chemical reactivity of the main molecules of Artemisia ansinthium, which causes interatomic interactions between the atoms of these molecules and the iron atoms of the mild steel surface, which reinforces the adsorption of our molecules.

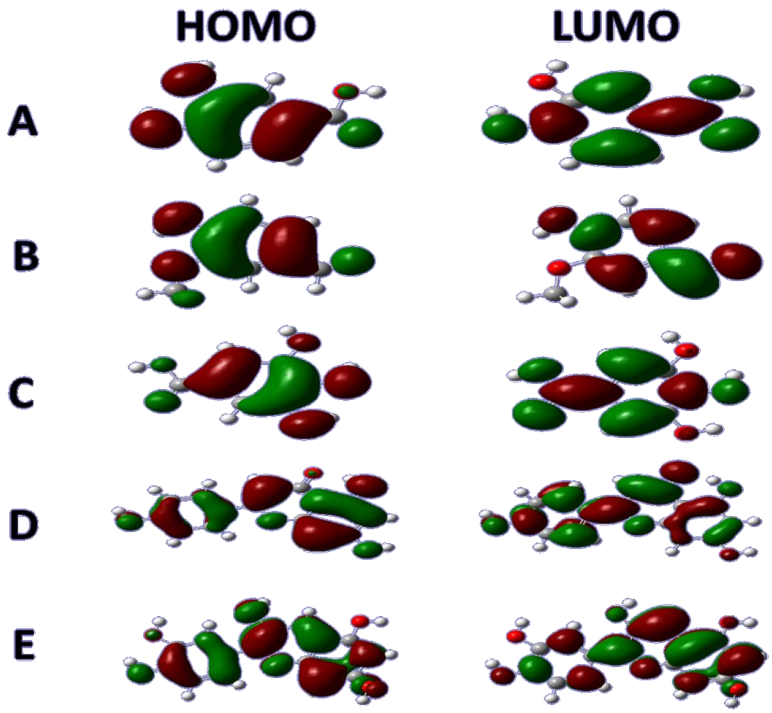

Figure 11. HOMO and LUMO molecular orbitals of 3,4-dihydroxybenzoic acid (A), vanillin (B), gallic acid (C), naringenin (D) and catechine (E) obtained with the DFT at B3LYP/6-31G (d,p) level

The HOMO and LUMO boundary orbitals of a molecule are important parameters for defining reactivity. A good correlation between E_{HOMO} and the efficiency of corrosion inhibition has been found, this energy is often associated with the electron donating capacity of the molecule [45]. A higher E_{HOMO} value means a good capacity of the inhibitor to yield its electrons to the vacant d-orbital of the metal. While a lower E_{HOMO} value is indicative of the ability of the inhibitor to acquire electrons from the metal orbitals by back-donation [46].

Indeed, the adsorption of inhibitor molecules on the metal surface occurs on the principle of donor-acceptor interactions between the vacant d orbitals of the metal atoms and the electrons of heterocyclic compounds [45]. Comparing the 5 major inhibitor compounds: A, B, C, D and E, the energy calculations show that compound E has the highest HOMO level (-4.845 eV) compared to those obtained for C (-6.252 ev), B (-6.262 ev), A (-6.304 ev) and D (-9.141 eV).

The global hardness (η) is defined as the resistance to electron cloud polarization or deformation under a small perturbation of the chemical reaction. A large energy gap corresponds to a hard molecule, while a soft molecule has a small energy gap which is an indication of low reactivity [47]. A remarkably less negative value of the Total Energy (-28025.873 ev) and a low value of ΔE (2.905 ev) for E which suggests a better reactivity compared to the other molecules, and it is classified as a soft molecule.

The electron capacity donation is determined by the number of transferred electrons (ΔN). We notice from our results that E has the highest ΔN value (0.975) which suggests its high electron donating capacity, followed by C (0.418), A (0.401), B (0.374) and finally D (-2.208). These results clearly justify that molecules of AQL inhibitor possess higher electron donating capacity than those of AQS inhibitor which therefore confirms the high inhibitory efficacy found by the gravimetric and electrochemical studies for AQL, it may be that the majority molecules of this extract react by synergy. The inhibitory efficiencies found by gravimetric and electrochemical techniques of AQL are higher than those of AQS, based on the results of theoretical calculations, possibly these differences may be related to the presence of catechin in AQL or a combined effect of gallic acid and catechin with 3,4-dihydroxybenzoic acid.

Table 6. The quantum descriptors of A, B, C, D and E calculated using DFT at B3LYB/6-31G (d, p)

Molecules	E_T (ev)	E_{HOMO} (ev)	E_{LUMO} (ev)	ΔE (ev)	χ	η	ΔN
A	-15542.868	-6.304	-1.311	4.992	3.807	2.496	0.401
B	-14564.593	-6.262	-1.618	4.644	3.94	2.322	0.374
C	-17589.478	-6.252	-1.296	4.956	3.774	2.478	0.418
D	-25948.691	-9.141	-1.974	7.167	5.557	3.583	-2.208
E	-28025.873	-4.845	-1.939	2.905	3.392	1.453	0.975

Alahiane et al. [48], found that 3,4-dihydroxybenzoic acid is a good stainless steel inhibitor in HCl solutions, indeed the maximum efficiency of 88% was obtained for an optimum inhibitor concentration of 10^{-2} M.

Vanillin is a molecule that has been proven by Emregül et al. [49], as a corrosion inhibitor for steel with an efficiency of 81.2% for a concentration of 0.01M in 2M HCl medium. It was

also found by El-Etre et al. [50] that vanillin acts as a good inhibitor of aluminum corrosion in a 5 M hydrochloric acid solution.

Gallic acid which is a compound present in henna extracts showed an inhibitory effect of mild steel in 1 M HCl [44]. Naringenin has been shown to inhibit the corrosion of aluminum and zinc against the aggressiveness of the acidic environment by its adsorption on the surface of the metals. Hussin et al. identify (+)-catechin hydrates as a good inhibitor of mild steel in 1M HCl medium, which acts as a mixed type inhibitor with predominance at the anode site [51].

4. CONCLUSION

Artemisia absinthium extracts have satisfactory results against the dissolution of mild steel in 1M HCl medium so they act as corrosion inhibiting agents, Indeed, at the concentration of 0.2 g/L, the protection efficiency was 85% for AQL and 82% for AQS. Both inhibitors demonstrated dual inhibitory action, which was classified as mixed type. Nyquist plots justified that the corrosion process is especially influenced by the charge transfer, which is confirmed by a single capacitive loop. The adsorption actions of these inhibitors in the acidic medium HCl 1M, obits to the Langmuir isotherm. The study by the different methods used shows a coherence of the results which confirms the complementarity of these methods. Surface analysis by SEM showed that damage caused by the acid media on the mild steel surface was reduced when AQL and AQS were used. Theoretically, a reasonable correlation was confirmed between the experiment results and the parameters obtained by the DFT method.

REFERENCES

[1] I.K. Ibrahim, and J.A. Naser, Plant Arch. 20 (2020) 3315.
[2] Y.L. Kobzar, and K. Fatyeyeva, Chem. Eng. J. 425 (2021) 131480.
[3] A.M. Abdel-Karim, and A.M. El-Shamy, J. Bio-Tribo-Corrosion 2022 82, 8 (2022) 1.
[4] D.Y. Wang, Z.G. Li, Y. Liu, H.J. Li, and Y.C. Wu, Corros. Sci. 208 (2022) 110609.
[5] A. Kadhim, G. Sulaiman, A.E. Abdel Moneim, R.M. Yusop, and A. Al-Amiery, J. Phys. Conf. Ser. 1795 (2021) 012011.
[6] N. Hossain, M.A. Chowdhury, A.K.M.P. Iqbal, M.S. Islam, N.Y. Sheikh Omar, and A.Z.A. Saifullah, Curr. Res. Green Sustain. Chem. 4 (2021) 100191.
[7] W.B.W. Nik, F. Zulkifli, R. Rosliza, and M.M. Rahman, Int. J. Mod. Eng. Res. 1 (2012) 723.
[8] A. Zargari, Medicinal Plants, Tehran University Press, Tehran, Iran, Volume 2 (1989) pp. 502-507.
[9] C.W. Wright, Artemisia medicinal and aromatic plants-Industrial Profiles, Chapter 1 (2002) 10.
[10] F.S. Sharopov, V.A. Sulaimonova, and W.N. Setzer, Rec. Nat. Prod. 6 (2012).

[11] E. Nibret, and M. Wink, Phytomedicine 17 (2010) 369.
[12] C.L. Chopra, M.C. Bhatia, and I.C. Chopra, J. Am. Pharm. Assoc. 49 (1960) 780.
[13] M.M. Zafab, M.E. Hamdard, and A. Hameed, J. Ethnopharmacol. 30 (1990) 223.
[14] S.G. Khattak, S.N. Gilani, and M. Ikram, J. Ethnopharmacol. 14 (1985) 45.
[15] F. Ahmad, R.A. Khan, S. Rasheed, and J. Islam. Acad. Sci. 5 (1992) 111.
[16] K.S. Bora, and A. Sharma, J. Pharm. Res. 3 (2010) 325.
[17] M. Mahmoudi, M.A. Ebrahimzadeh, F. Ansaroudi, S.F. Nabavi, and S.M. Nabavi, African J. Biotechnol. 8 (2009).
[18] M. Yadav, R.R. Sinha, T.K. Sarkar, and N. Tiwari, J. Adhes. Sci. Technol. 29 (2015) 1690.
[19] Q. Wang, H. Zheng, L. Liu, Q. Zhang, X. Wu, Z. Yan, Y. Sun, and X. Li, Ind. Crops Prod. 188 (2022) 115640.
[20] M.F. Heragh, and H. Tavakoli, J. Mol. Struct. 1245 (2021) 131086.
[21] A. Salcı, H. Yüksel, and R. Solmaz, J. Taiwan Inst. Chem. Eng. 134 (2022) 104349.
[22] R.S.A. Hameed, A.M. Nassar, M.M. Badr, R.S.A. Hameed, M.M. Aljohani, A.B. Essa, A. Khaled, S.R. Al-Mhyawi, and M.S. Soliman, Int. J. Electrochem. Sci. 16 (2021) 210446.
[23] L. Koursaoui, Y. Kerroum, M. Tabyaoui, A. Guenbour, A. Bellaouchou, B. Satrani, M. Ghanmi, I. Warad, A. Chaouch, and A. Zarrouk, Biointerface Res. Appl. Chem. 11 (2021) 10119.
[24] M. Afrokh, S. Baroud, Y. Kerroum, A. Hatimi, and S. Tahrouch, Biointerface Res. Appl. Chem. 12 (2022) 7075.
[25] B.S. Mahdi, M.K. Abbass, M.K. Mohsin, W.K. Al-azzawi, M.M. Hanoon, M.H.H. Al-kaabi, L.M. Shaker, A.A. Al-amiery, W.N.R.W. Isahak, A.A.H. Kadhum, and M.S. Takriff, Mol. 27 (2022) 4857.
[26] M. Damej, R. Hsissou, A. Berisha, K. Azgaou, M. Sadiku, M. Benmessaoud, N. Labjar, and S. El hajjaji, J. Mol. Struct. 1254 (2022) 132425.
[27] F. Benhiba, H. Zarrok, A. Elmidaoui, E. Hezzat, R. Touir, A. Guenbour, A. Zarrouk, S. Boukhris, and H. Oudda, J. Mater. Environ. Sci. 6 (2015) 2301.
[28] O. Craciunescu, D. Constantin, A. Gaspar, L. Toma, E. Utoiu, and L. Moldovan, Chem. Cent. J. 6 (2012) 1.
[29] S. Kordali, R. Kotan, A. Mavi, A. Cakir, A. Ala, and A. Yildirim, J. Agric. Food Chem. 53 (2005) 9452.
[30] Y.J. Lee, M. Thiruvengadam, I.M. Chung, and P. Nagella, Aust. J. Crop Sci. 7 (2013) 1921.
[31] I. Koyuncu, Cell. Mol. Biol. 64 (2018) 25.
[32] J. Iqbal, World J. Pharm. Res. 1 (2012) 796.
[33] K. Msaada, N. Salem, O. Bachrouch, S. Bousselmi, S. Tammar, A. Alfaify, K. Al Sane,

W. Ben Ammar, S. Azeiz, A. Haj Brahim, M. Hammami, S. Selmi, F. Limam, and B. Marzouk, J. Chem. (2015).

[34] E.N. Sal'nikova, N.F. Komissarenko, A.I. Derkach, S.E. Dmitruk, and G.I. Kalinkina, Chem. Nat. Compd. 29 (1993) 678.

[35] G. Zengin, A. Mollica, A. Aktumsek, C. Marie Nancy Picot, and M. Fawzi Mahomoodally, Eur. J. Integr. Med. 12 (2017) 135.

[36] M. Ali, B.H. Abbasi, and Ihsan-ul-haq, Ind. Crops Prod. 49 (2013) 400.

[37] B.E.A. Rani, and B.B.J. Basu, Int. J. Corros. (2012).

[38] A. Döner, R. Solmaz, M. Özcan, and G. Kardaş, Corros. Sci. 53 (2011) 2902.

[39] M. Zhu, Z. He, L. Guo, R. Zhang, V.C. Anadebe, I.B. Obot, and X. Zheng, J. Mol. Liq. 342 (2021) 117583.

[40] R. Haldhar, D. Prasad, L.T.D. Nguyen, S. Kaya, I. Bahadur, O. Dagdag, and S.C. Kim, Mater. Chem. Phys. 267 (2021) 124613.

[41] F. Mansfeld, Corrosion. 37 (1981) 301.

[42] A.D. Mercer, Br. Corros. J. 25 (1990) 246.

[43] W.J. Lorenz, Dechema Monographs (1986) 101.

[44] A. Ostovari, S.M. Hoseinieh, M. Peikari, S.R. Shadizadeh, and S.J. Hashemi, Corros. Sci. 51 (2009) 1935.

[45] V. Saraswat, M. Yadav, and I.B. Obot, Colloids Surfaces A 599 (2020) 124881.

[46] S. Xia, M. Qiu, L. Yu, F. Liu, and H. Zhao, Corros. Sci. 50 (2008) 2021.

[47] V.S. Sastri, and J.R. Perumareddi, Corros. 53 (1997).

[48] M. Alahiane, R. Oukhrib, A. Berisha, Y.A. Albrimi, R.A. Akbour, H.A. Oualid, H. Bourzi, A. Assabbane, A. Nahlé, and M. Hamdani, J. Mol. Liq. 328 (2021) 115413.

[49] K.C. Emregül, and M. Hayvali, Mater. Chem. Phys. 83 (2004) 209.

[50] A.Y. El-Etre, Corros. Sci. 43 (2001) 1031.

[51] M.H. Hussin, and M.J. Kassim, Int. J. Electrochem. Sci. 6 (2011) 1396.